NASA TECHNICAL MEMORANDUM

NASA TM X-1811

NASA TM X-1811

THE LIQUID-VAPOR INTERFACE DURING OUTFLOW IN WEIGHTLESSNESS

by Steven G. Berenyi and Kaleel L. Abdalla

Lewis Research Center

Cleveland, Ohio

NATIONAL AERONAUTICS AND SPACE ADMINISTRATION • WASHINGTON, D. C. • JUNE 1969

NASA TM X-1811

THE LIQUID-VAPOR INTERFACE DURING OUTFLOW IN WEIGHTLESSNESS

By Steven G. Berenyi and Kalell L. Abdalla

Lewis Research Center
Cleveland, Ohio

NATIONAL AERONAUTICS AND SPACE ADMINISTRATION

For sale by the Clearinghouse for Federal Scientific and Technical Information
Springfield, Virginia 22151 – CFSTI price $3.00

ABSTRACT

An experimental program was conducted to determine the effect of outflow from a tank on the behavior of the liquid-vapor interface in weightlessness. A previously determined correlation was extended to larger tank models in a high Weber number flow region. The tests were conducted with two separate tank shapes and two test liquids, and at various initial fillings.

THE LIQUID-VAPOR INTERFACE DURING OUTFLOW IN WEIGHTLESSNESS

by Steven G. Berenyi and Kaleel L. Abdalla

Lewis Research Center

SUMMARY

An experimental program was conducted to determine the effect of outflow from a tank on the behavior of the liquid-vapor interface in a weightless environment. A correlation, obtained for small model tanks, has been extended in the high Weber number region to larger models by the use of the 5- to 10-Second Zero-Gravity Facility at Lewis. Two different tank shapes, three tank sizes, and two test liquids were used in conducting the experiments. Additional data have been obtained to determine the effect of initial filling on the interface distortion during outflow.

INTRODUCTION

During studies of outflow from containers in a weightless environment, it was determined that the liquid-vapor interface distorted from its initial hemispherical configuration (refs. 1 and 2). In reference 2 this distortion was found to be primarily a function of outflow velocity. Although these studies indicated that the distortion can be correlated by the Weber number, the experiments were limited to a range of tank sizes of less than 4 centimeters in radius by facility time limitations.

The object of this investigation was to extend the data of reference 2 to larger tank sizes (up to 15-cm radius) by the use of the new 5- to 10-Second Zero-Gravity Facility. The effect of outflow on the distortion of the liquid-vapor interface is presented here in a form similar to reference 2. The data are also presented and compared in a form used by reference 3. References 4 to 7 are included as a summary of related low-gravity outflow problems. In addition, the effect of initial liquid filling on the distortion of the interface is discussed in more detail.

SYMBOLS

h	centerline distance from liquid-vapor interface to outlet, cm
R	tank radius, cm
V	liquid-vapor interface velocity in weightlessness, cm/sec
V_m	mean liquid velocity, cm/sec
We	Weber number, $We = \rho V_m^2 R/4\sigma$
β	specific surface tension, cm^3/sec^2
μ	viscosity, g/cm-sec
ρ	liquid density, g/cm^3
σ	surface tension, dyne/cm

APPARATUS AND PROCEDURE

The facility and the experiment vehicle employed in this study along with the procedures for their operation, are described in detail in the appendix.

Test Tanks and Liquids

The test tanks for the experiments in this program were 4-, 7.5-, and 15-centimeter radius cylinders. Two bottom shapes were included, a hemispherical shape with a center outlet and an inverted elliptical shape with a side outlet. The configurations are shown in figure 1. The tanks were machined from acrylic plastic and polished clear for photographic purposes. As shown, each tank was equipped with inlet baffles to reduce the effect of the incoming pressurant on the liquid interface. The baffles were stainless-steel discs 1.0 tank radius in diameter and positioned 0.5 tank radius below the pressurant inlet port. The tank outlets were all square edged and had radii equal to 1/10 tank radius. The outlet tube lengths were equal to 10 outlet radii. The pressurant inlet baffle and the liquid outlet port geometries were sized and positioned to maintain similarity with the test apparatus of reference 2.

Test liquids were chosen to simulate rocket propellants under similar conditions. The surface tension to density ratio and the 0^o liquid-to-solid contact angle were considered the most important properties for these tests. These and other pertinent properties of the test liquids are listed in table I.

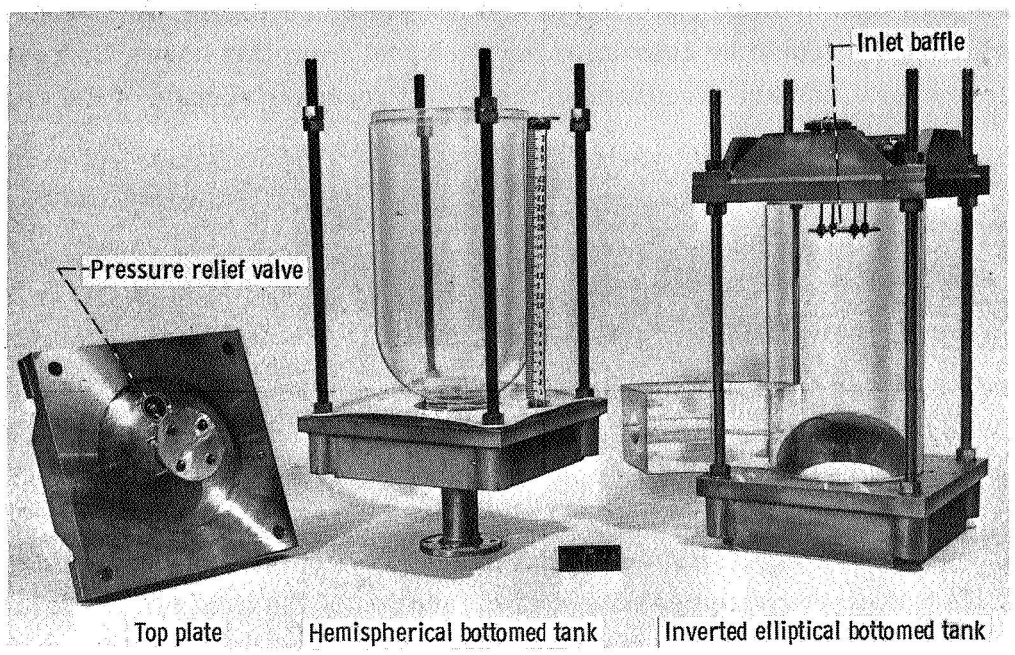

Figure 1. - Test tank configurations.

TABLE I. - PROPERTIES OF TEST LIQUIDS

[Contact angle with cast acrylic plastic in air, 0°.]

Liquid	Surface tension at 20° C, σ, dynes/cm	Density at 20° C, ρ, g/cm^3	Viscosity at 20° C, μ, g/cm-sec	Specific surface tension, β, cm^3/sec^2
Anhydrous ethanol	22.3	0.789	1.2×10^{-2}	28.3
Trichloro-trifluoro-ethane	18.6	1.579	0.7×10^{-2}	11.8

Data Reduction

The motion of the liquid-vapor interface during outflow was recorded for each test on high-speed color film. The flow rates during the tests were obtained from telemetered records of both operating pressures and flowmeter readings. An average or mean outflow velocity V_m could be calculated for each test from this known flow rate. Details of these operations are discussed in the Test Procedure section of the appendix.

RESULTS AND DISCUSSION

Outflow Characteristics

The scope of this investigation included the test variables of outflow velocity, tank shape, tank size, test fluid, and initial filling level. A set of data points was obtained by varying the mean outflow velocities in a range of about 5 to 20 centimeters per second for several combinations of the other test variables.

The results of a typical outflow test during weightlessness are presented in figure 2 in the form of a time-displacement curve of the motion of the liquid-vapor interface along the tank centerline. When a partially filled cylindrical container is exposed to weightlessness the liquid-vapor interface oscillates about its hemispherical equilibrium shape for a short time period. In this test sufficient time was allowed, after placing the system in a weightless environment, for the interface to reach its lowest point in its first

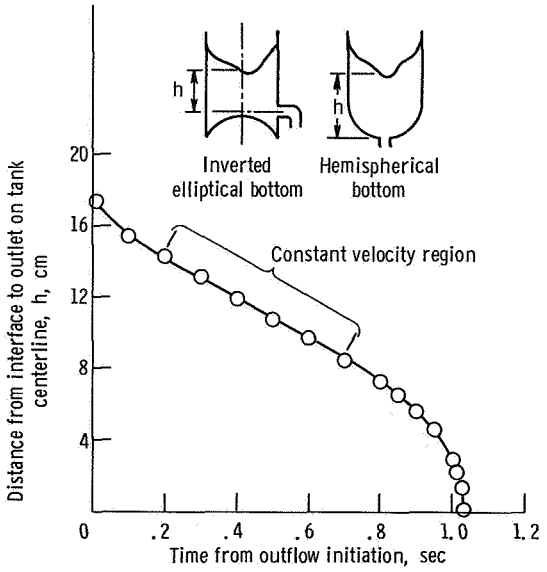

Figure 2. - Motion of liquid-vapor interface on tank centerline for typical outflow test during weightlessness.

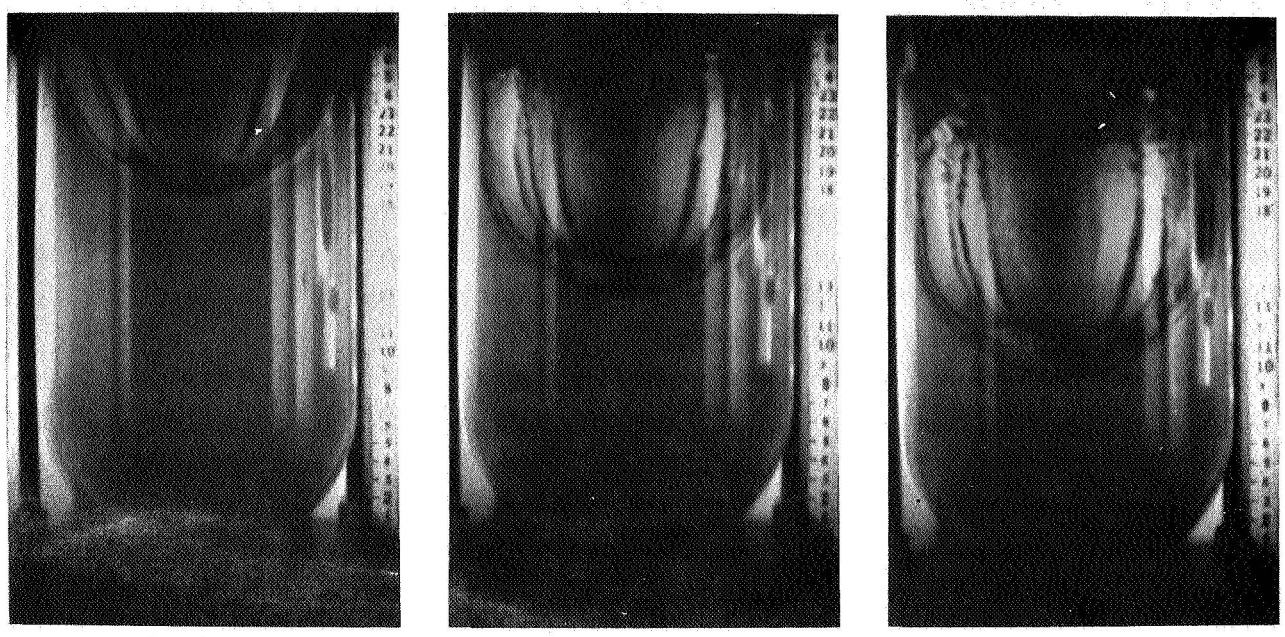

(a) Time, 0 second. (b) Time, 0.4 second. (c) Time, 0.6 second.

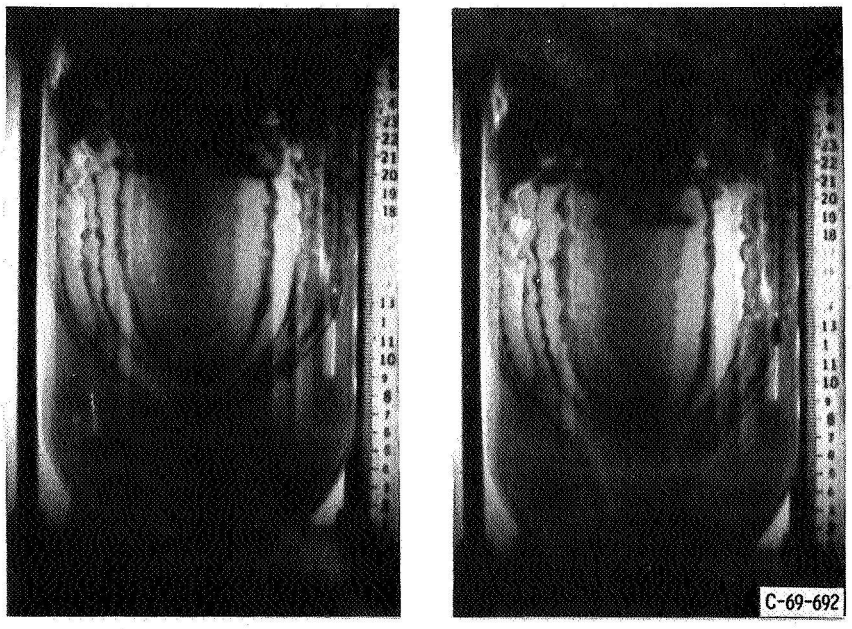

(d) Time, 0.8 second. (e) Vapor ingestion; time, 0.92 second.

Figure 3. - Liquid-vapor interface distortion during outflow from tank in weightlessness. Mean outflow velocity, 11.8 centimeters per second; hemispherical bottomed 7.5-centimeter-radius tank.

oscillation, at which time outflow was initiated (T = 0, fig. 2). After a startup transient the interface velocity becomes constant, followed by acceleration of the interface toward the outlet until vapor ingestion occurs. This study is concerned with the steady-state outflow phenomenon associated with the "constant velocity region" shown in figure 2.

A sequence of photographs (fig. 3) is included showing the motion of the interface during the outflow phenomenon investigated. The initial hemispherical interface can be observed in figure 3(a). Upon initiation of outflow the interface shape changes slightly as shown in the next picture (fig. 3(b)). As the outflow continues, the entire interface moves towards the outlet; however, no further change in the shape of the interface is observed (fig. 3(c)). This is the constant velocity region designated in figure 2. When the interface reaches the vicinity of the outlet, the centerline starts to accelerate (fig. 3(d)) resulting in vapor ingestion (fig. 3(e)).

The interface velocities obtained from the time displacement curves are compared with their respective mean velocities in figure 4. This method of presentation was used in reference 3, and data from it are included for comparison. On this figure the dashed line represents the case where $V = V_m$; that is, the velocity of the interface on the tank centerline is the same as the mean velocity based on outflow rate and tank cross-sectional area. At lower velocities the interface velocity approaches the mean velocity but deviates from it as V_m is increased. It is significant to note that this deviation from the mean reaches a limiting value. The solid line on the figure, drawn through the data for the 4- and 7.5-centimeter-radius tanks, is parallel to the reference line and indicates this higher limit. This increase in velocity along the tank centerline above V_m tends to distort the shape of the original hemispherical interface.

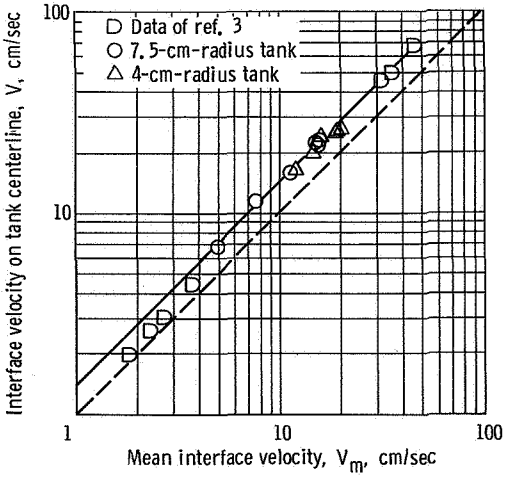

Figure 4. - Interface velocity during outflow in weightlessness. Test liquid, ethanol.

Liquid-Vapor Interface Distortions with 3-Tank-Radii Initial Filling

Derdul (ref. 2) also noted the trends discussed above and correlated the distortion of the interface with a dimensionless Weber number grouping. The results of this present investigation are presented in a similar manner.

A distortion parameter, defined in reference 2 as $(V - V_m)/V$, and a Weber number, $We = \rho V_m^2 R/4\sigma$ are used for the correlation. The distortion parameter may be considered as a measure of the deviation of the interface from its normal zero-gravity hemispherical shape. The Weber number is essentially a ratio of the inertia (velocity) forces to the capillary (surface tension) forces, and may be used as an indication of the disturbance imposed on the interface during outflow.

Interface distortions in 4- and 7.5-centimeter-radius tanks. - Shown in figure 5 are the results of this investigation along with the correlating line of reference 2 for an initial filling of 3 tank radii. In this study, as well as in reference 2, the liquid height from the center of the tank outlet to the normal-gravity flat liquid-vapor interface is defined as the initial filling. The data points are for 4- and 7.5-centimeter-radius hemispherical bottomed tanks. Although the correlating line was shown in reference 2 to be valid for flat, hemispherical, and inverted elliptical bottomed tanks, the majority of that data was obtained for 1-, 2-, and 4-centimeter-radius flat bottomed tanks. It is evident from figure 5 that the data of this present investigation for 4- and 7.5-centimeter-radius tanks extends this correlating relation in the high Weber number (inertia dominated) region for the larger tank sizes studied. The limiting value of 0.27 for the distortion observed by Derdul for smaller tanks remains the same for tank sizes up to twice the radius originally tested. The data scatter, which is well within the range of reference 2, may be attributed to experimental error introduced in the operation and regulation of the pumping system. The trend exhibited by the correlation of reference 2 is identical to that of figure 4; that

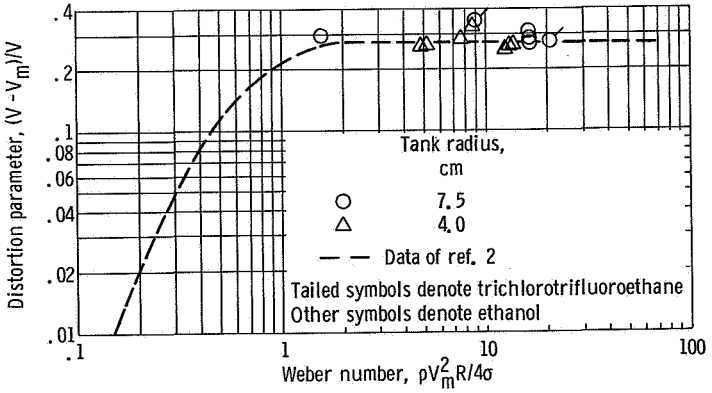

Figure 5. - Effect of outflow on distortion of liquid-vapor interface in hemispherical bottomed cylindrical tanks at initial filling of 3 tank radii.

is, increasing V_m for a particular tank configuration caused the distortion parameter to increase up to a limiting value and any further increase had no effect on the distortion.

Interface distortions in a 15-centimeter-radius tank. - Additional tests were conducted with a 15-centimeter-radius hemispherically bottomed tank. For this large size, the time required for the centerline of the liquid-vapor interface to reach its low point in the formation cycle was too great to allow an outflow test in the 5 seconds available. For this reason, the outflow in the 15-centimeter tank could not be initiated at this low point as for the other tank sizes. In this case a compromise starting time had to be selected. This compromise time occurred when the low point of the interface was stationary, although the remainder of the interface was moving. At the initiation of outflow, this low point was not on the tank centerline as in the smaller tanks (see fig. 6). For all tests, the low point of the liquid-vapor interface was stationary at the initiation of outflow. The initial interface shape, however, for the 15-centimeter radius tank tended to be relatively flat compared to the ideal hemispherical equilibrium shape.

As outflow progressed, the interface low point moved from the initial position shown in figure 6 to the tank centerline, after which time the low point remained on the centerline. For this tank the distortion parameters were evaluated using the low point velocity. The results presented in figure 7 indicate that although there is considerable scatter in the data, the distortions are lower than shown by the previous correlation. It is possible that this difference in distortions was due to the initial interface shape. However, because of the difference in the evaluation technique, it may not be valid to make quantitative comparisons. Even though the initial conditions differed somewhat, it is worthy to

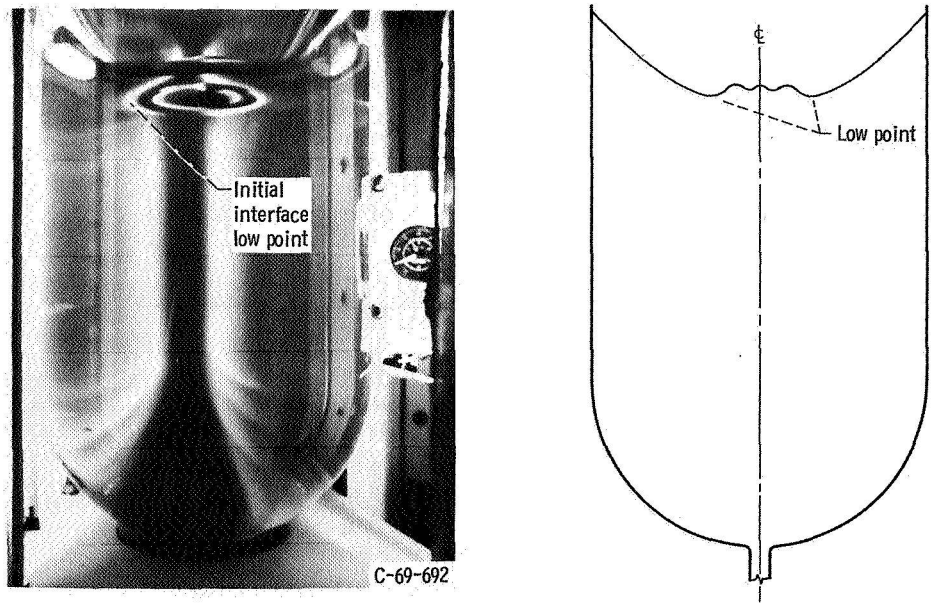

Figure 6. - Liquid-vapor interface shapes for 15-centimeter-radius tank.

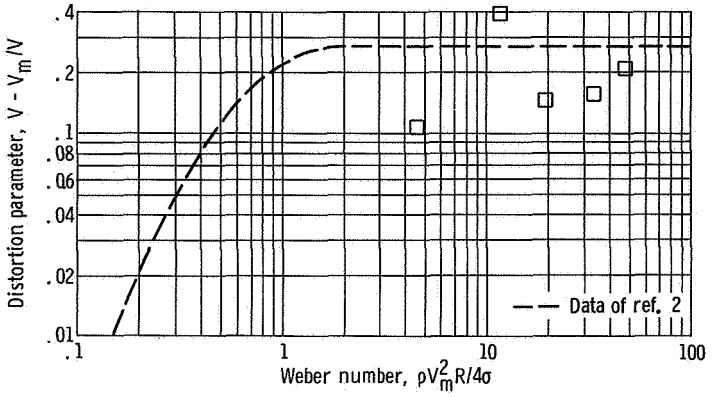

Figure 7. - Effect of outflow on distortion of liquid-vapor interface in hemispherical bottomed, 15-centimeter-radius cylindrical tanks. Initial filling, 3 tank radii, test liquid, ethanol.

note that visual observation of the interface behavior in tank sizes approximately four times as great as previously tested did not reveal any major differences in the outflow phenomenon. However, longer test times would be necessary to make an accurate quantitative evaluation of the interface distortion.

Effect of Initial Filling

Previous investigators have noted an effect of initial filling on the magnitude of distortion observed during outflow. Derdul has presented data at various initial fillings, part of which is reproduced here in figure 8. His data were for flat bottomed cylindrical

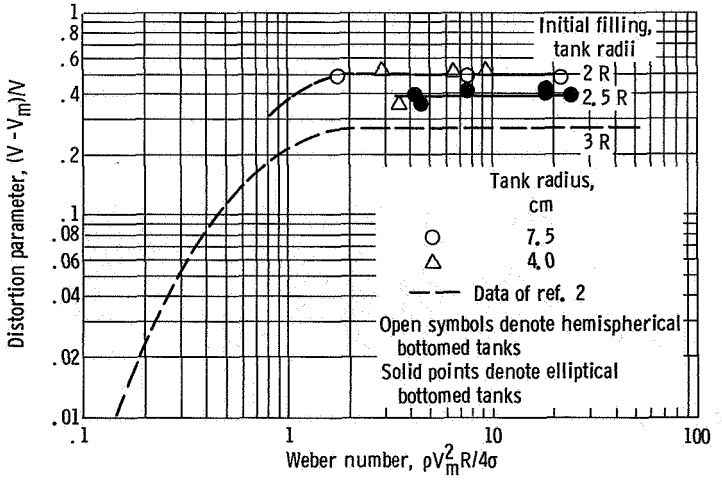

Figure 8. - Effect of initial filling on distortion of liquid-vapor interface in cylindrical tanks during outflow.

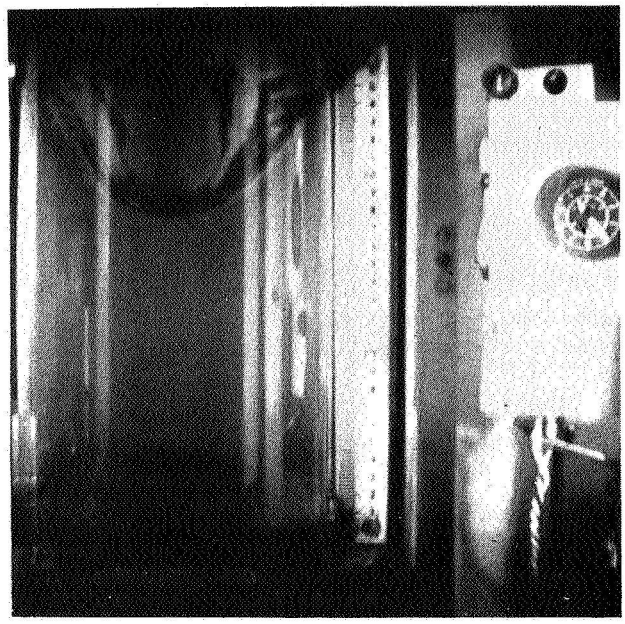

(a) Time, 0 second.

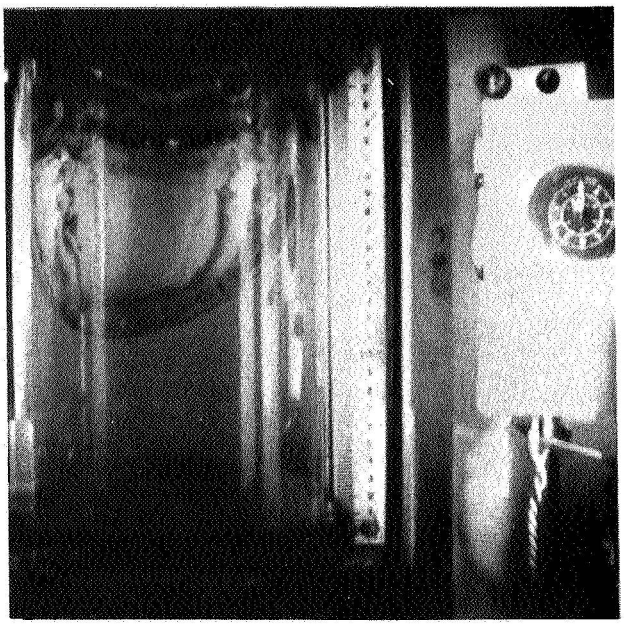

(b) Time, 0.4 second.

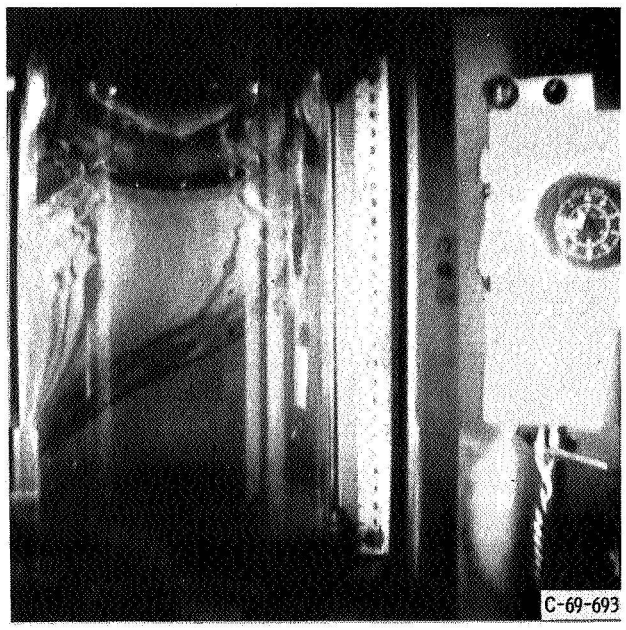

(c) Vapor ingestion; time, 0.6 second.

Figure 9. - Liquid-vapor interface distortion during outflow from inverted elliptical bottomed, 7.5-centimeter-radius tank in weightlessness. Mean outflow velocity, 12.0 centimeters per second.

tanks. As a further extension of his work, data points were obtained with both hemispherical and inverted elliptical bottomed tanks of larger diameters.

Data were obtained for 2-tank-radii initial fillings with hemispherical bottomed tanks of 4- and 7.5-centimeter radii and compared with the data of reference 2. The additional data points obtained in this study for the larger tanks do fit Derdul's original curve. A series of test drops was also made with both the inverted elliptical and the hemispherical bottomed tank with an initial filling of 2.5 radii. Figure 9 illustrates the interface shape at various times during outflow from the elliptical bottomed tank. In determining the distortion parameter for this tank configuration only the axial component of the weightless interface velocity was used. This method was successfully used in the data correlations of reference 2. These data points also fall where expected; that is, between the 2- and 3-radii-filling data points. It is evident from this limited amount of data that the interface distortion during outflow is definitely a function of the initial liquid filling. Higher initial fillings resulted in lower values of distortion. However, it should be noted that these three fillings alone are not sufficient to derive any functional relation describing the exact nature of the effect of filling.

SUMMARY OF RESULTS

An experimental study of the liquid-vapor interface behavior during outflow from partially filled cylindrical tanks was conducted in a weightless environment. The tests were run with three tank sizes, two tank shapes, and two test liquids having 0° contact angle. The results obtained indicate the following:

1. The correlation of the interface distortion with a Weber number was extended to larger tank sizes in the high outflow velocity (inertia dominated) flow region.

2. Even though the test tank radius was increased to 7.5 centimeters, the interface distortion parameter reached the same limiting value of 0.27 as originally determined for smaller tanks (with initial fillings of 3R).

3. For the 15-centimeter-radius tank, accurate measurements of distortion could not be made in the 5 seconds of test time available. Visual observations of outflow in these tanks, however, indicate no marked deviations from the phenomenon observed in the smaller tanks.

4. The data obtained for the 7.5-centimeter-radius tanks confirmed the dependence of the distortion parameter upon initial liquid filling. As before, outflow from higher initial fillings resulted in lower distortions.

Lewis Research Center,
National Aeronautics and Space Administration,
Cleveland, Ohio, February 19, 1969,
124-09-17-01-22.

APPENDIX - APPARATUS AND PROCEDURE

Test Facility

The experimental data for this study were obtained in the Lewis Research Center's 5- to 10-Second Zero-Gravity Facility. A schematic diagram of this facility is shown in figure 10. The facility consists of a concrete-lined 8.5-meter- (28-ft-) diameter shaft that extends 155 meters (510 ft) below ground level. A steel vacuum chamber, 6.1 meters (20 ft) in diameter and 143 meters (470 ft) high, is contained within the concrete shaft. The pressure in this vacuum chamber is reduced to 13.3 newtons per square meter (1.3×10^{-4} atm) by utilizing the Center's wind tunnel exhaust system and an exhauster system located in the facility.

The ground-level service building has, as its major elements, a shop area, a control room, and a clean room. Assembly, servicing, and balancing of the experiment vehicle are accomplished in the shop area. Tests are conducted from the control room (see fig. 11) which contains the exhauster control system, the experiment vehicle predrop checkout and control system, and the data retrieval system. Those components of the experiment which are in contact with the test fluid are prepared in the facility's Class 10 000 clean room. The major elements of the clean room are an ultrasonic cleaning system (fig. 12(a)) and a Class 100 laminar-flow work station (fig. 12(b)) for preparing those experiments requiring more than normal cleanliness.

Mode of operation. - The Zero-Gravity Facility has two modes of operation. One is to allow the experiment vehicle to free-fall from the top of the vacuum chamber which results in nominally 5 seconds of free-fall time. The second mode is to project the experiment vehicle upwards from the bottom of the vacuum chamber by a high-pressure pneumatic accelerator located on the vertical axis of the chamber. The total up-and-down trajectory of the experiment vehicle results in nominally 10 seconds of free-fall time. The 5-second mode of operation was used for this experimental study.

In either mode of operation, the experiment vehicle falls freely. That is, no guide wires, electrical lines, etc., are connected to the vehicle. Therefore, the only force (aside from gravity) acting on the freely falling experiment vehicle is due to residual-air drag. This results in an equivalent gravitational acceleration acting on the experiment which is estimated to be of the order of 10^{-5} g maximum.

Recovery system. - After the experiment vehicle has traversed the total length of the vacuum chamber, it is decelerated in a 3.6-meter- (12-ft-) diameter, 6.1-meter- (20-ft-) deep container which is located on the vertical axis of the chamber and filled with small pellets of expanded polystyrene. The deceleration rate (averaging 32 g) is controlled by the flow of pellets through the area between the experiment vehicle and the wall of the deceleration container. This deceleration container is mounted on a cart which can be retracted prior to utilizing the 10-second mode of operation. In this mode

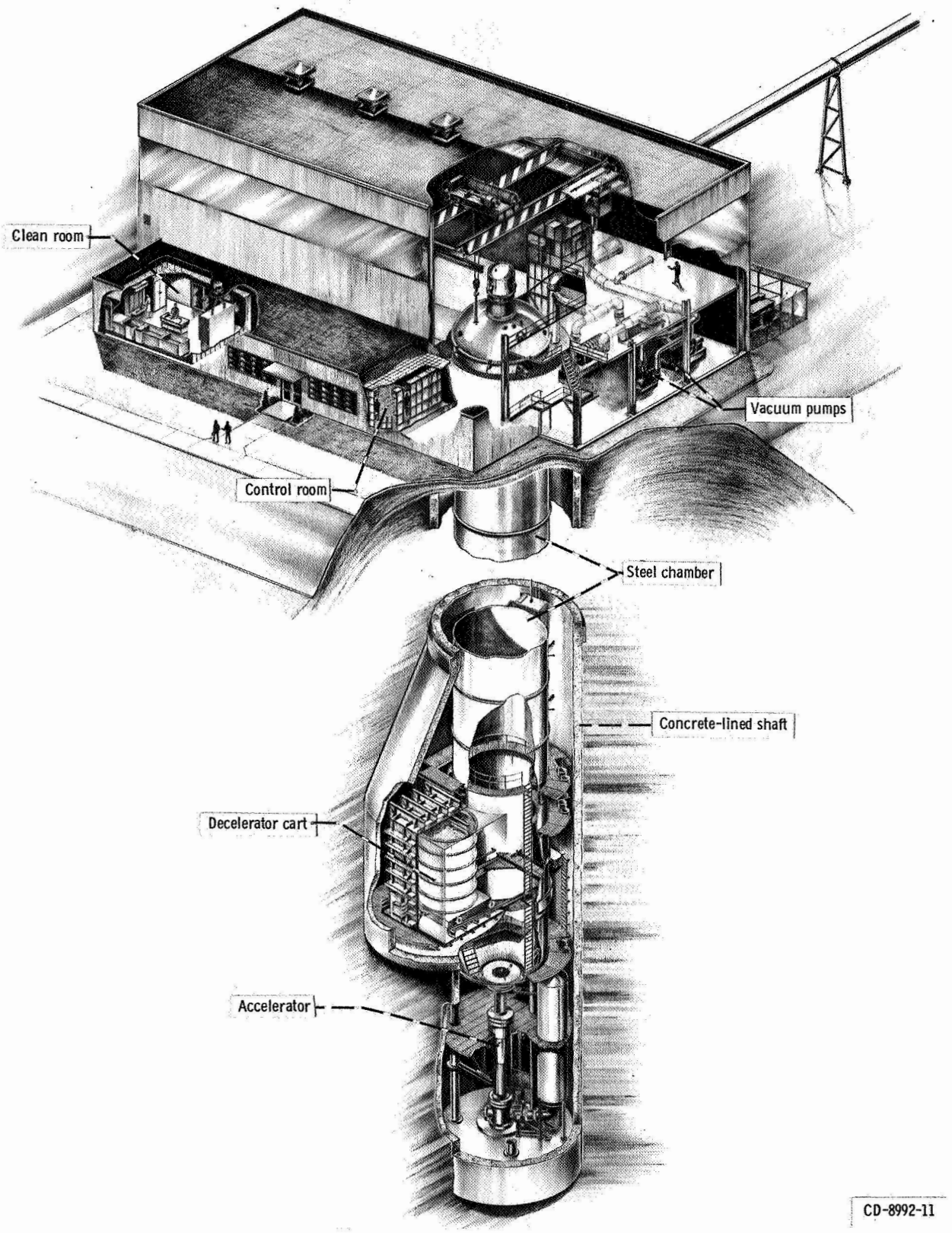

Figure 10. - Schematic diagram of 5- to 10-Second Zero-Gravity Facility.

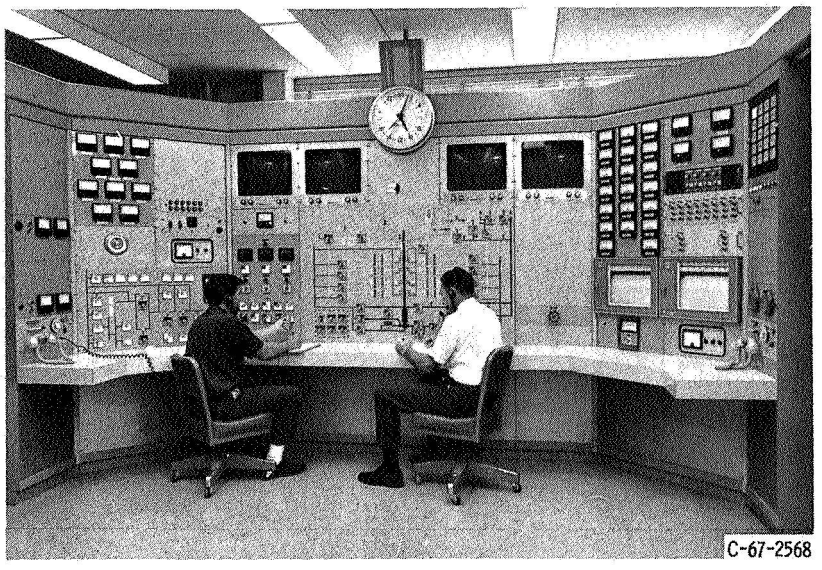

Figure 11. - Control room.

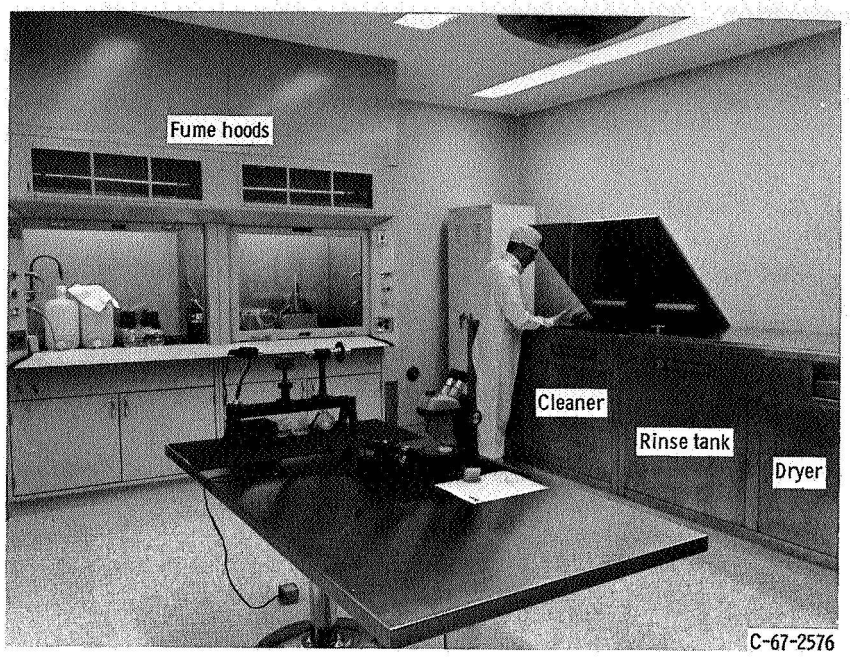

(a) Ultrasonic cleaning system.

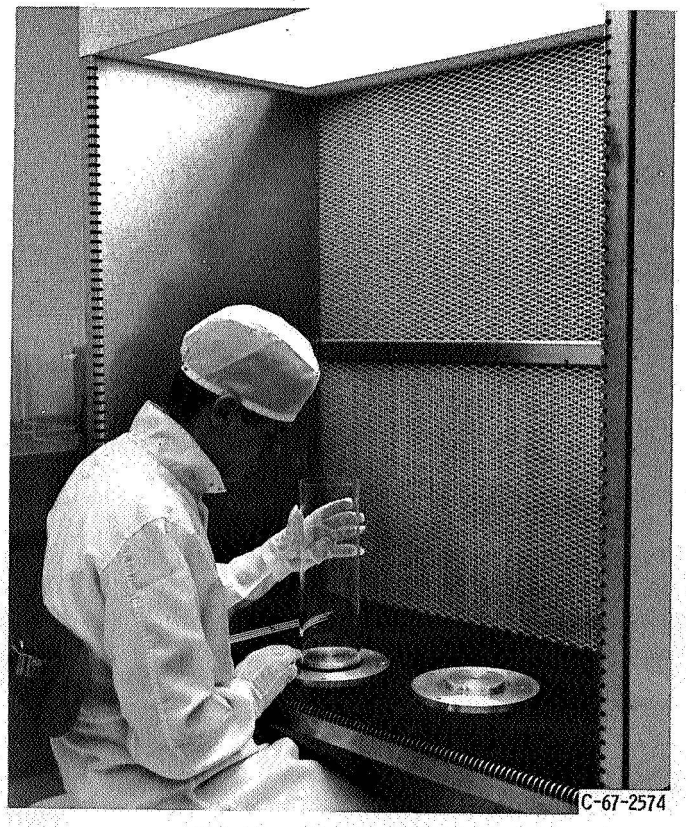

(b) Laminar-flow work station.

Figure 12. - Clean room.

of operation, the cart is deployed after the experiment vehicle is projected upward by the pneumatic accelerator. The deceleration container mounted on the cart is shown in the photograph of figure 13.

Experiment Vehicle

The experiment vehicle used to obtain the data for this study is shown in figure 14. The overall vehicle height (exclusive of the support shaft) is 3.0 meters (9.85 ft) and the largest diameter is 1.06 meters (3.5 ft). The vehicle consists of a telemetry system section contained in the aft fairing and an experiment section which is housed in the cylindrical midsection.

Telemetry system. - The on-board telemetry system which is used to collect pressure and flow rate data is a standard Inter-Range Instrumentation Group (IRIG) FM/FM 2200-megahertz telemeter. It is used during a test drop to record up to 18 channels of continuous data. The system has a frequency range up to 2100 hertz. The telemetered

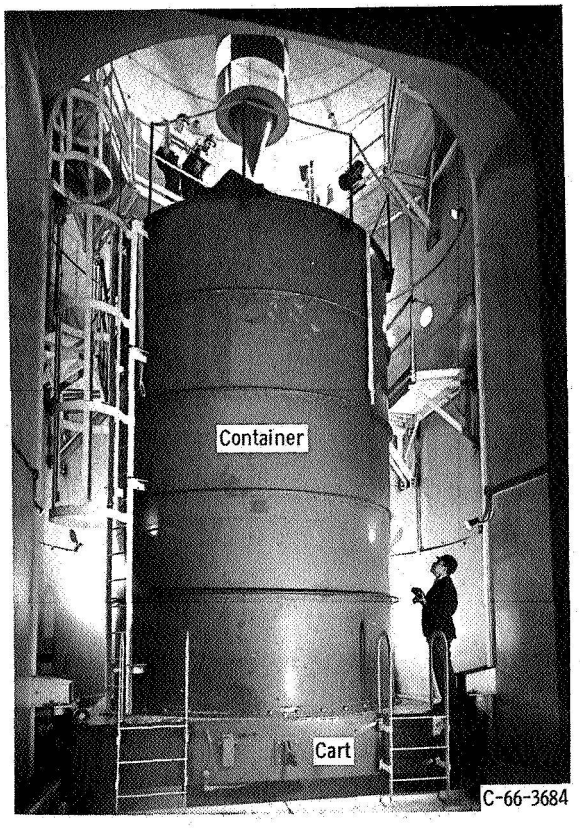

Figure 13. - Deceleration system.

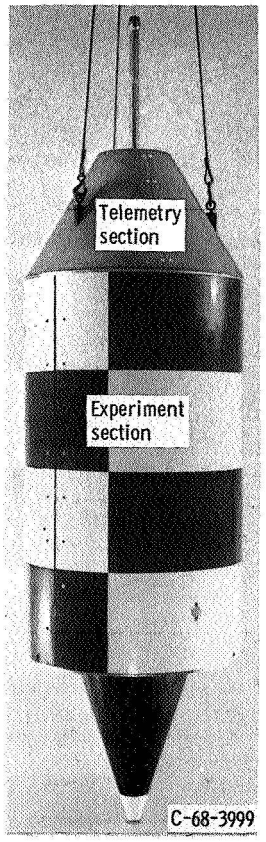

Figure 14. - Experiment vehicle.

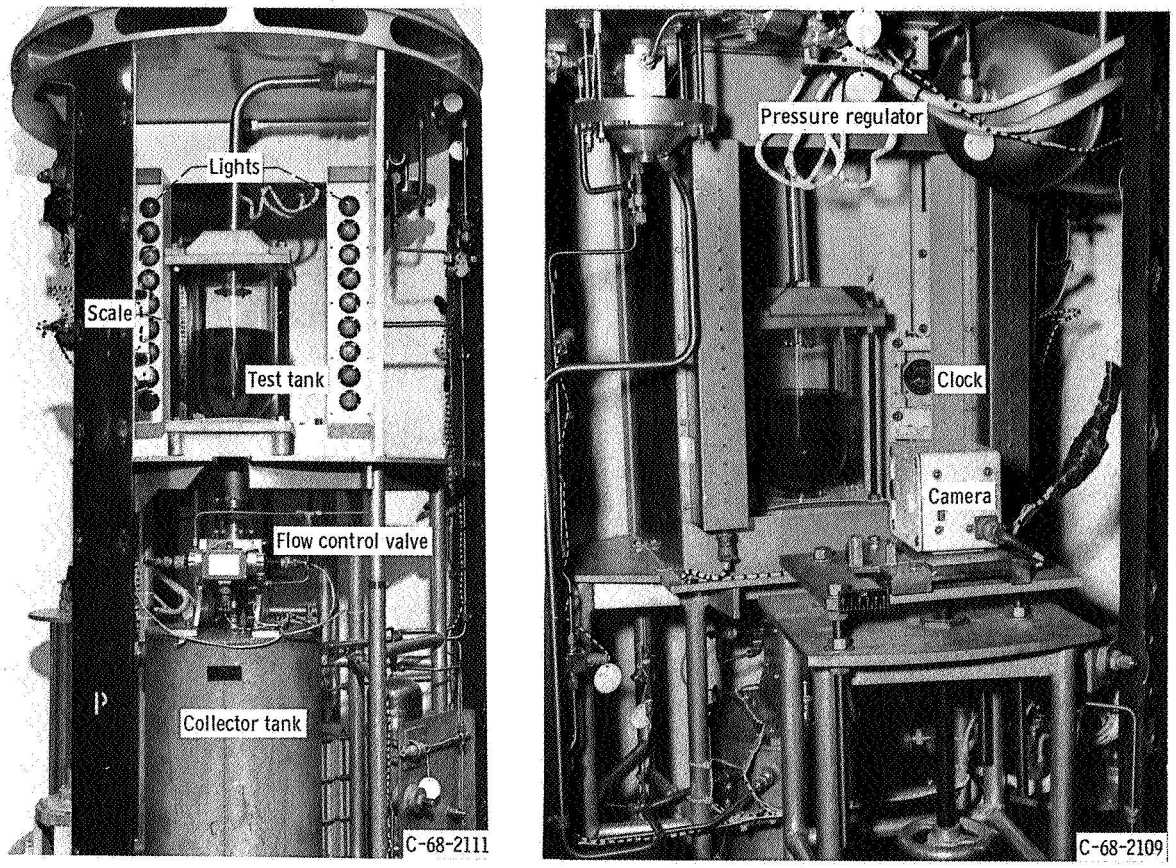

Figure 15. - Experiment section details.

data are recorded on two high-response recording oscillographs located in the control room.

Experiment. - The experiment section consists of the test tank, the pressurization and flow control system, and the necessary photographic equipment. Figure 15 shows the details of the experiment section. The test tank is mounted in the vehicle so that the motion of the liquid-vapor interface can be recorded by a high-speed motion-picture camera. A centimeter scale and a sweep hand clock are located in the camera's field of view. This clock has an accuracy of ±0.005 second. For the photography, the experiment is lighted with an array of spotlights.

The pressurization and flow control system is illustrated schematically in figure 16. Shown on the figure are the various components used for outflow regulation. The differential pressure is maintained by the pressure regulator during outflow from the test tank and is continuously recorded by telemetry.

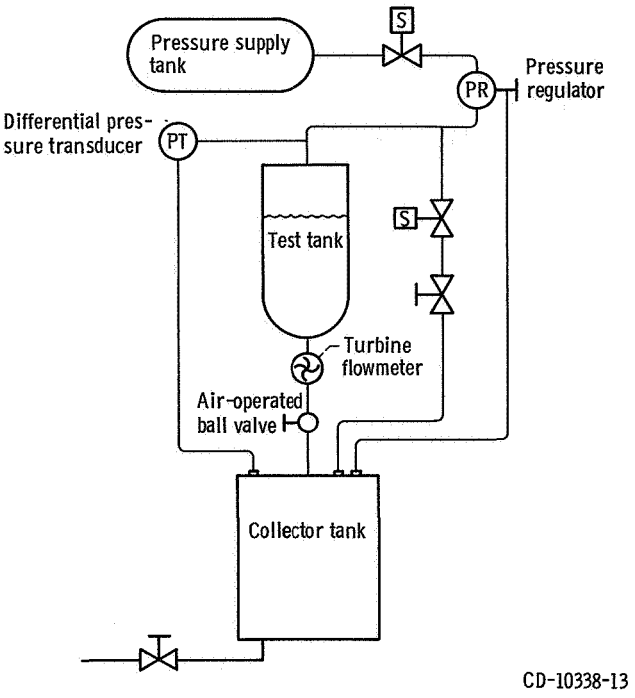

Figure 16. - Pressurization and flow control system.

Test Procedure

Before any experimental data point was obtained, the test tank was thoroughly washed, ultrasonically cleaned, hot-air dried, and assembled in the clean room. The tank was then installed in the experiment vehicle and filled to the proper level with the test liquid.

The liquid velocity and the time of outflow initiation were set for each test drop. The required velocity was obtained by regulating the pressure across the test tank. A fast-acting ball valve located in the outlet line was used to initiate flow from the pressurized tank. To determine a pressure against velocity curve for the system, normal-gravity flow calibration tests were conducted. The measurements for these calibrations were made by photographically recording the motion of the interface during normal-gravity draining, from which a velocity could be calculated, and also recording the output from a turbine flowmeter placed in the outlet line (see fig. 16). The two methods agreed to within ±1 percent. The differential pressure between the vapor space above the surface and the collector tank was also recorded. These normal-gravity calibrations, however, included the velocity caused by static head. Once a correction had been made to eliminate this effect, the proper pressure could be set for the zero-gravity free-fall tests.

The precise time for outflow initiation (the interface formation time) was determined from observations of the motion of the liquid-vapor interface upon entering weightlessness in previous drops with no outflow. As the system enters weightlessness, the interface oscillates about its equilibrium hemispherical shape. The time when the interface reached a low point in the first cycle of its oscillation was used for initiation of outflow. At this time the velocity of the low point on the interface is zero.

The vehicle was positioned at the top of the vacuum chamber as shown in figure 17. It was suspended by the support shaft on a hinged-plate release mechanism. During vacuum chamber pumpdown and prior to release, monitoring of experiment vehicle systems was accomplished through an umbilical cable attached to the top of the support shaft. Electrical power was supplied from ground equipment. The system was then switched to internal power a few minutes before release. The umbilical cable was remotely pulled from the support shaft 0.5 second prior to release. The vehicle was released by pneumatically shearing a bolt that was holding the hinged-plate in the closed position. No measurable disturbances were imparted to the experiment vehicle by this release procedure.

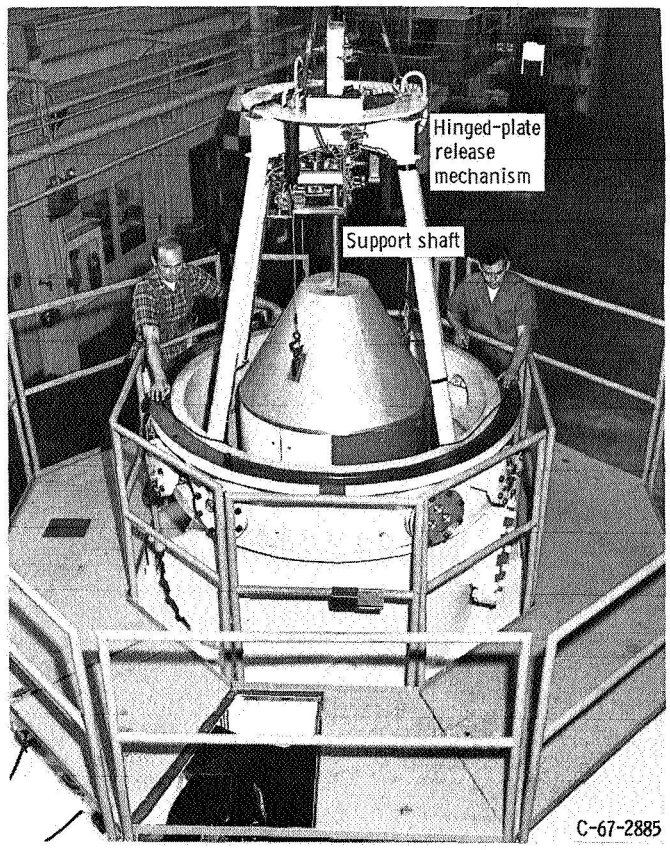

Figure 17. - Vehicle position prior to release.

The total free-fall test time obtained in this mode of operation is 5.16 seconds. During the test drop the vehicle's trajectory and deceleration were monitored on closed-circuit television. Following the test drop, the vacuum chamber was vented to the atmosphere and the experiment vehicle was returned to ground level (see fig. 18).

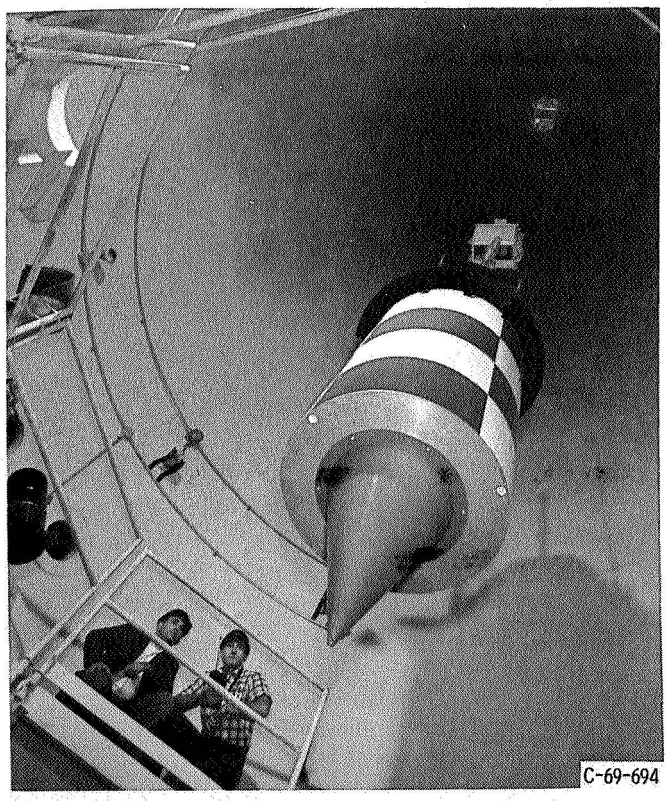

Figure 18. - Experiment vehicle being returned to ground level.

REFERENCES

1. Nussle, Ralph C.; Derdul, Joseph D.; and Petrash, Donald A.: Photographic Study of Propellant Outflow From a Cylindrical Tank During Weightlessness. NASA TN D-2572, 1965.

2. Derdul, Joseph D.; Grubb, Lynn S.; and Petrash, Donald A.: Experimental Investigation of Liquid Outflow from Cylindrical Tanks During Weightlessness. NASA TN D-3746, 1966.

3. Otto, E. W.: Static and Dynamic Behavior of the Liquid-Vapor Interface During Weightlessness. Chem. Eng. Prog. Symp. Ser., vol. 62, no. 61, 1966, pp. 158-177.

4. Abdalla, Kaleel L.; and Berenyi, Steven G.: Vapor Ingestion Phenomenon in Weightlessness. NASA TN D-5210, 1969.

5. Grubb, Lynn S.; and Petrash, Donald A.: Experimental Investigation of Interfacial Behavior Following Termination of Outflow in Weightlessness. NASA TN D-3897, 1967.

6. Lacovic, Raymond F.; and Stofan, Andrew J.: Experimental Investigation of Vapor Ingestion in the Centaur Liquid Hydrogen Tank. NASA TM X-1482, 1968.

7. Gluck, D. F.; Gille, J. P.; Simkin, D. J.; and Zukoski, E. E.: Distortion of the Liquid Surface During Tank Discharge Under Low G Conditions. Chem. Eng. Prog. Symp. Ser., vol. 62, no. 61, 1966, pp. 150-157.

NATIONAL AERONAUTICS AND SPACE ADMINISTRATION
WASHINGTON, D.C. 20546

OFFICIAL BUSINESS

FIRST CLASS MAIL

POSTAGE AND FEES PAID
NATIONAL AERONAUTICS AND
SPACE ADMINISTRATION

POSTMASTER: If Undeliverable (Section 158
Postal Manual) Do Not Return

"The aeronautical and space activities of the United States shall be conducted so as to contribute . . . to the expansion of human knowledge of phenomena in the atmosphere and space. The Administration shall provide for the widest practicable and appropriate dissemination of information concerning its activities and the results thereof."

—NATIONAL AERONAUTICS AND SPACE ACT OF 1958

NASA SCIENTIFIC AND TECHNICAL PUBLICATIONS

TECHNICAL REPORTS: Scientific and technical information considered important, complete, and a lasting contribution to existing knowledge.

TECHNICAL NOTES: Information less broad in scope but nevertheless of importance as a contribution to existing knowledge.

TECHNICAL MEMORANDUMS: Information receiving limited distribution because of preliminary data, security classification, or other reasons.

CONTRACTOR REPORTS: Scientific and technical information generated under a NASA contract or grant and considered an important contribution to existing knowledge.

TECHNICAL TRANSLATIONS: Information published in a foreign language considered to merit NASA distribution in English.

SPECIAL PUBLICATIONS: Information derived from or of value to NASA activities. Publications include conference proceedings, monographs, data compilations, handbooks, sourcebooks, and special bibliographies.

TECHNOLOGY UTILIZATION PUBLICATIONS: Information on technology used by NASA that may be of particular interest in commercial and other non-aerospace applications. Publications include Tech Briefs, Technology Utilization Reports and Notes, and Technology Surveys.

Details on the availability of these publications may be obtained from:

SCIENTIFIC AND TECHNICAL INFORMATION DIVISION

NATIONAL AERONAUTICS AND SPACE ADMINISTRATION

Washington, D.C. 20546